Physica 14D (1985) 305–326
North-Holland, Amsterdam

AN EXPLORATION OF THE HÉNON QUADRATIC MAP

Donald L. HITZL and Frank ZELE
Lockheed Palo Alto Research Laboratory, Advanced Systems Studies, Dept. 92-20, Bldg. 205 (D.L.H.) and Electro-Optics Laboratory, Dept. 95-41, Bldg. 201 (F.Z.), 3251 Hanover Street, Palo Alto, California 94304, USA

Received 22 May 1984

The two-dimensional mapping, introduced by Hénon in 1976, which yields a strange attractor for the parameter values $a = 1.4$, $b = 0.3$ has been investigated over the extended region $-2 \le a \le 6$, $-1 \le b \le 1$. Analytical solutions have been obtained for the onset of real stable cycles of periods 1 through 6. The associated bifurcations to stable cycles of twice the period (2 to 12) have also been determined. All the resulting boundary curves are displayed in the a, b parameter plane. Finally, an interesting three-dimensional generalization of the Hénon map is announced.

1. Introduction

Recently, there has been an explosion of interest in (and understanding of) the long-term behavior of deterministic dynamical systems. Much of the recent work has emphasized the large-scale irregular or chaotic solutions which can occur in even very simple nonlinear systems [1–6]. Of particular interest has been the period doubling mechanism [2] leading to the onset of chaos in both conservative and dissipative dynamical systems. The universal features inherent in one dimensional maps, originally discovered by Feigenbaum, have been described very clearly in [4].

The fundamental new object which has emerged from the study of the long-term behavior of solution trajectories for dissipative dynamical systems is called a strange attractor – a term originally due to Ruelle [3]. This is a set, in an appropriate space, which attracts solution trajectories towards itself but exhibits a strong instability along the (very complicated) attracting structure. This instability manifests itself in the sensitive dependence to initial conditions characteristic of chaotic behavior in deterministic dynamical systems.

Probably one of the simplest mathematical models yielding strange attractors is given by the following two-dimensional quadratic map T:

$$\begin{aligned} x_{i+1} &= 1 + y_i - a x_i^2, \\ y_{i+1} &= b x_i. \end{aligned} \tag{1}$$

This map was invented by Hénon in 1976 [7]; see also [3] and [4] for descriptions.

Because of its extreme elegance and analytical simplicity, the Hénon quadratic map T has been the subject of a wide variety of further investigations [7–14] and also has been used as a basic model problem in, for example, the development of new theory concerned with the fractal dimension D of the resulting strange attractors [15, 16]. Concurrently, many other 1 and 2-dimensional maps have also been studied – see, for example [17–20].

The purpose of this paper is to explore the general behavior of the Hénon quadratic map T at the opposite extreme from the well-known chaotic sequence of iterates yielding a strange attractor at the parameter values $a = 1.4$, $b = 0.3$. Here, we will present analytical and numerical results for the existence and stability of low-order periodic sequences of iterates of T. (For differentiable dynamical systems, our results are exactly analogous

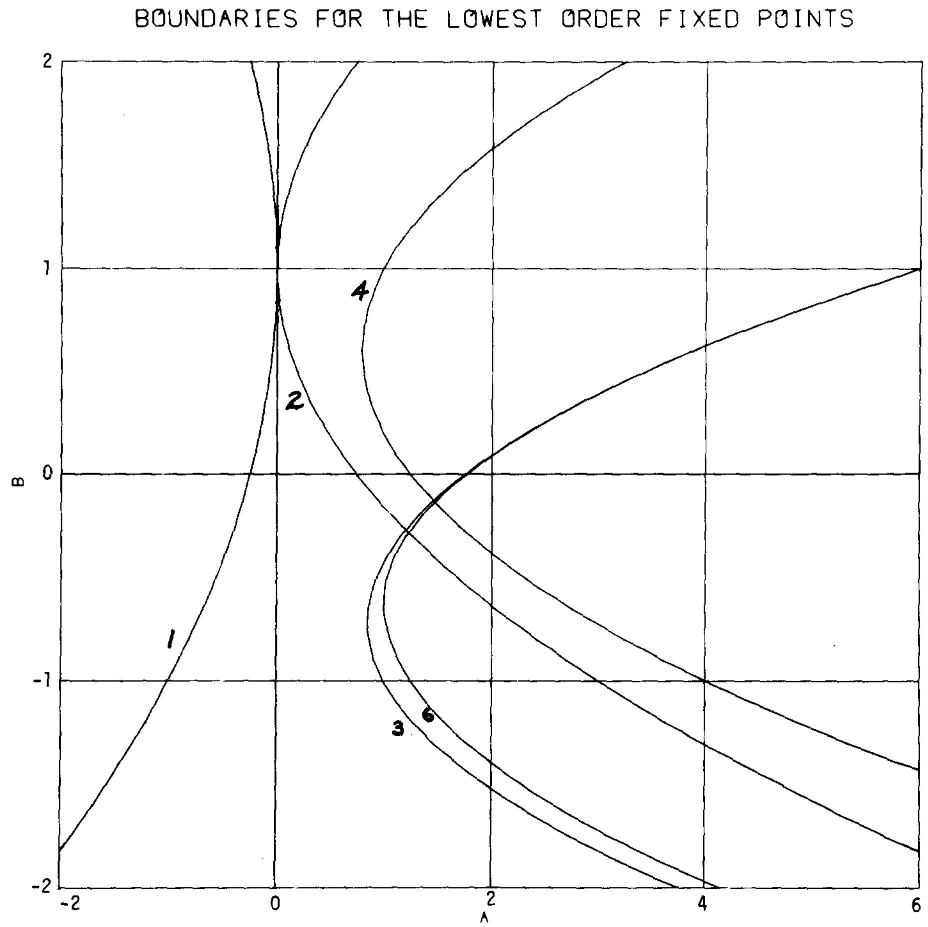

Fig. 1. Boundaries in the a, b parameter plane for the emergence of real stable cycles of periods 1, 2, 3, 4, and 6.

to the determination of critical periodic orbits delineating the boundary between stability and instability.) Furthermore, these periodic sequences, of period $P = 1$ to 6, have been obtained in analytical form throughout the entire dissipative region $(-1 < b < 1)$ yielding contraction of areas [7,13] and also at the conservative (or area-preserving) limit values $b = \pm 1$.

The analytical developments needed to achieve closed-form expressions for the fixed points will be discussed briefly and the resulting boundary curves, in the a, b parameter space, will be presented. We begin with period 1 and proceed, step by step, to period 6.

2. Period 1 fixed points

The development of a stable cycle of period $P = 1$ has been presented already by Hénon in [7]. However, in order to have a consistent notation and a completely self-contained exposition, we will begin by repeating this analysis. Recast (1) in the form of a 1D, two-step recurrence,

$$x_{i+2} = 1 + bx_i - ax_{i+1}^2. \tag{2}$$

Since every iterate is identical, drop the index i and define† $z \triangleq ax$ so

$$z^2 + (1 - b)z - a = 0. \tag{3}$$

†The symbol $\triangleq$ denotes *equality by definition*.

The solution to this quadratic is

$$2z = -(1-b) \pm \sqrt{\Delta_1}, \tag{4}$$

where

$$\Delta_1 \triangleq 4a + (1-b)^2 \geq 0 \tag{5}$$

in order for two real fixed points to exist for $P = 1$. Eq. (5) determines the left most boundary curve shown in fig. 1. To the left of this boundary curve $\Delta_1 = 0$, there are no longer any real fixed points. We also note that, for each of the boundary curves shown in fig. 1, real cycles emerge on the right of the curves.

Throughout this paper, we will be concerned with real stable cycles of periods 1 to 6. Hence, the stability of the fixed points will be examined for each cycle. For the cycle of $P = 1$, linearizing (1) in the neighborhood of the fixed point x gives the matrix M and eigenvalue equation

$$|M - \lambda I| \triangleq \begin{vmatrix} -2ax - \lambda & 1 \\ b & -\lambda \end{vmatrix} = \lambda^2 + 2ax\lambda - b = 0, \tag{6}$$

where we have stability for $|\lambda| < 1$ and critical cycles when $|\lambda| = 1$. Since this eigenvalue equation will be obtained for each period P from 1 through 6, eq. (6) will be written in the following general form:

$$\lambda^2 + \Sigma\lambda + (-b)^P = 0 \tag{7}$$

and, for $P \geq 2$, only the expression for Σ will be given.

If we set $\lambda = -1$ in (6), we obtain the boundary curve

$$\Delta_2 \triangleq 4a - 3(1-b)^2 = 0 \tag{8}$$

for the onset of real stable cycles of $P = 2$. This curve is labelled 2 in fig. 1. Hence, the results of the stability analysis for $P = 1$ can now be stated as follows:

i) The point corresponding to the minus sign in (4) is always unstable.
ii) The point corresponding to the plus sign in (4) is stable between $\Delta_1 = 0$, $\Delta_2 = 0$ and $|b| = 1$; it is unstable elsewhere.

We note that a cycle of any period P is never stable if $|b| > 1$ for then we have expansion, rather than contraction, of area as the mapping T is iterated. However, an expanded scale, $-2 \leq b \leq 2$, is used in fig. 1 so that the behavior of the boundary curves $\Delta_1 = 0$ to $\Delta_6 = 0$ is available over a larger region.

Finally, for both eigenvalues to be real, the discriminant in (6), $a^2x^2 + b \equiv z^2 + b \geq 0$. By using (4) for z, the boundary relation

$$a = -b \pm (1-b)\sqrt{-b} \tag{9}$$

is easily obtained. This limiting curve (9) is shown in fig. 2 surrounded on each side by the curves $\Delta_1 = 0$ and $\Delta_2 = 0$. The eigenvalues are complex in the shaded region for $b \leq 0$ and real otherwise.

The significance of real eigenvalues is that successive iterates of the mapping approach the stable fixed point along the direction (eigenvector) appropriate to the eigenvalue of larger absolute value. For complex eigenvalues, successive iterates spiral into the stable fixed point.

3. Period 2 fixed points

For a period 2 cycle, there are a total of $2^2 = 4$ fixed points of which 2 are simply the $P = 1$ cycle repeated twice. In fact, as shown in either (1) or (2), each iteration of the map introduces the square of the current x value. Hence, for a cycle of period P, we expect to find a total of 2^P fixed points.

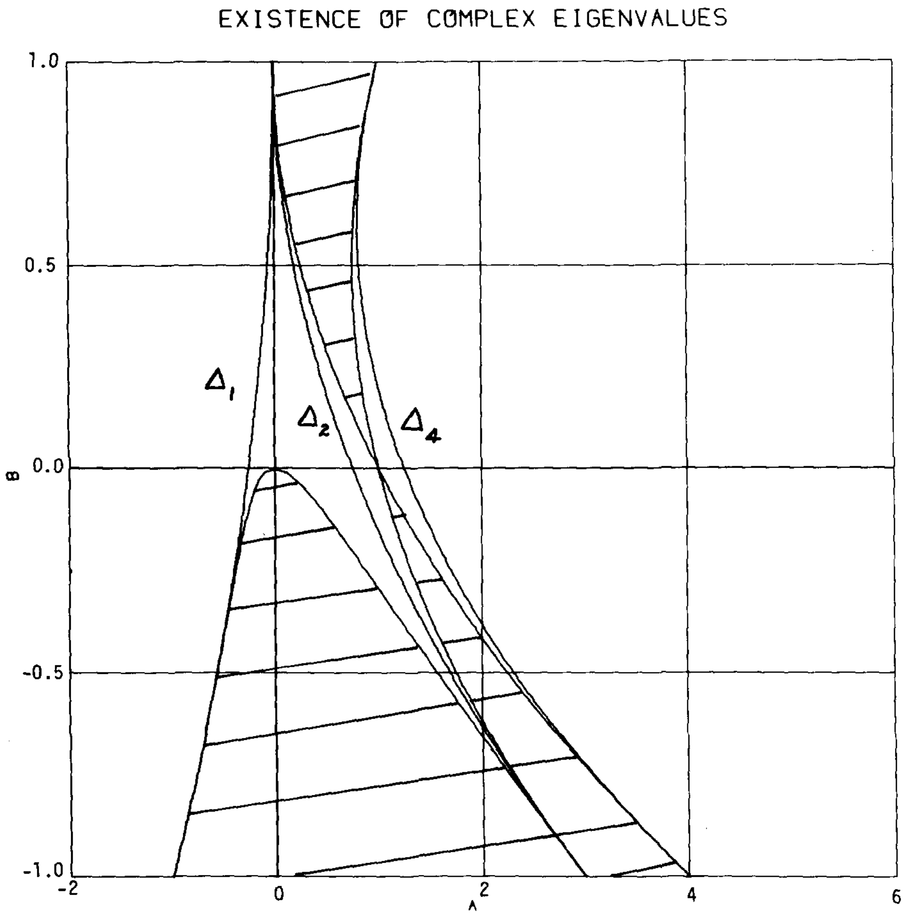

Fig. 2. Boundary curves for the existence of complex eigenvalues for periods 1 and 2.

Now, for the remaining two fixed points of period 2, we have

$$\begin{aligned} &ax_0^2+(1-b)x_1-1=0, \\ &ax_1^2+(1-b)x_0-1=0, \end{aligned} \tag{10}$$

where $x_0 \neq x_1$ and $x_2 \equiv x_0$. Subtract the second equation of (10) from the first and obtain

$$a(x_0+x_1)=(1-b), \tag{11}$$

so the fundamental variable z, which will always be defined as the mean of the x_i times a,

$$z \triangleq \frac{1}{P} a \sum_i x_i \tag{12}$$

is given here by

$$z=\tfrac{1}{2}a(x_0+x_1)=\tfrac{1}{2}(1-b). \tag{13}$$

Using (11) to eliminate x_1 in the first of (10) gives

$$\begin{aligned} &2ax_0=(1-b)+\sqrt{\Delta_2} \\ &\text{and} \\ &2ax_1=(1-b)-\sqrt{\Delta_2} \end{aligned} \tag{14}$$

for the two fixed points of $P=2$. For these to be real, Δ_2 given in (8) must satisfy $\Delta_2 \geq 0$. For the stability analysis of the cycle with $P=2$, the matrix M is given by

$$M = \begin{bmatrix} -2ax_1 & 1 \\ b & 0 \end{bmatrix} \begin{bmatrix} -2ax_0 & 1 \\ b & 0 \end{bmatrix} \tag{15}$$

and the eigenvalue equation $|M - \lambda I| = 0$ takes the form (7) with

$$\Sigma = -2(2a^2 x_0 x_1 + b). \tag{16}$$

Now, from (14) and (8), we have

$$a^2 x_0 x_1 = (1-b)^2 - a, \tag{17}$$

so, setting $\lambda = -1$ in the eigenvalue equation, we get

$$\Delta_4 \triangleq 4a - 5 + 6b - 5b^2 \geq 0 \tag{18}$$

for the existence of real stable $P = 4$ fixed points. The curve $\Delta_4 = 0$ is shown in both figs. 1 and 2 and gives the right-hand boundary for the existence of stable fixed points of $P = 2$. A detailed stability analysis then yields the result that the $P = 2$ cycle is stable between $\Delta_2 = 0$, $\Delta_4 = 0$ and $|b| = 1$. The cycle is unstable elsewhere.

We consider now where in the a, b parameter space the $P = 2$ eigenvalues will be real. Using (17), the discriminant in (7) is given by

$$\left[2(1-b)^2 - 2a + b\right]^2 - b^2 \geq 0. \tag{19}$$

This factors into the two terms

$$(1 - 2b + b^2 - a)(1 - b + b^2 - a) \geq 0, \tag{20}$$

which delineate the boundary between real and complex eigenvalues for $P = 2$. The region with complex eigenvalues is shown shaded in fig. 2 and is again sandwiched between the curves $\Delta_2 = 0$ and $\Delta_4 = 0$.

Data for the emergence of stable cycles of periods 1 and 2 is given in table I for a set of values of b in the interval $-1 \leq b \leq 1$. The single fixed point x_0 is also tabulated.

Table I
Emergence of stable cycles of periods 1 and 2

Period	a	b	x_0
1	0.0	1.0	∞
2	0.0	1.0	∞
1	−0.0625	0.5	4.0
2	0.1875	0.5	1.333...
1	−0.1225	0.3	2.8571
2	0.3675	0.3	0.9524
1	−0.25	0.0	2.0
2	0.75	0.0	0.666...
1	−0.4225	−0.3	1.5385
2	1.2675	−0.3	0.5128
1	−0.5625	−0.5	1.333...
2	1.6875	−0.5	0.444...
1	−1.0	−1.0	1.0
2	3.0	−1.0	0.333...

4. Period 3 fixed points

For a cycle of period 3, there are a total of $2^3 = 8$ fixed points. Two are simply the $P = 1$ fixed points repeated three times. Hence, there remain 6 fixed points which form two separate cycles. Using (2), the governing equations are

$$\begin{aligned} &ax_0^2 + x_1 - bx_2 - 1 = 0, \\ &ax_1^2 + x_2 - bx_0 - 1 = 0, \\ &ax_2^2 + x_0 - bx_1 - 1 = 0. \end{aligned} \tag{21}$$

First, we define

$$\xi \triangleq \tfrac{1}{3}\sum_i x_i, \quad z \triangleq a\xi, \quad \eta \triangleq \tfrac{1}{3}\sum_i x_i^2 \tag{22}$$

and find the remarkably simple relation

$$a\eta + (1-b)\xi - 1 = 0. \tag{23}$$

Next, we note that, if we can find the equation we want it will be of the form

$$x^3 - \alpha x^2 + \beta x - \gamma = (x - x_0)(x - x_1)(x - x_2) = 0, \tag{24}$$

where the elementary symmetric functions α, β, γ are

$$\alpha = x_0 + x_1 + x_2 = 3\xi,$$
$$\beta = x_0x_1 + x_0x_2 + x_1x_2 = \tfrac{1}{2}(\alpha^2 - 3\eta), \tag{25}$$
$$\gamma = x_0x_1x_2.$$

So, the idea was to use eqs. (21) to formulate expressions for α, β, γ in terms of ξ and η and ultimately, using (23), obtain a single relation in terms of ξ.

This can be done. Consider

$$\begin{aligned}\alpha\beta &= \tfrac{3}{2}\xi(9\xi^2 - 3\eta)\\ &= (x_0^2x_1 + x_1^2x_2 + x_2^2x_0)\\ &\quad + (x_0^2x_2 + x_1^2x_0 + x_2^2x_1) + 3\gamma\\ &\triangleq f_1(\xi, \eta, a, b) + f_2(\xi, \eta, a, b) + f_3(\xi, \eta, a, b).\end{aligned} \tag{26}$$

We can easily construct the f_j above from eqs. (21). As a single example

$$f_1 = \frac{3}{a}\left[\xi - \left(\frac{b}{2} + 1\right)\eta + \frac{3}{2}b\xi^2\right]. \tag{27}$$

Ultimately we obtain from (26) the quartic

$$\begin{aligned}&9z^4 + 6(1-b)z^3 - (10a + 1 - 8b + b^2)z^2\\ &\quad + 2(1-b)(a + 1 + b + b^2)z\\ &\quad + a[a - 2(1 + b + b^2)] = 0\end{aligned} \tag{28}$$

in terms of the fundamental variable z. This quartic contains the cycle of $P = 1$ as a redundant solution. Hence, if we divide (3) into (28), the desired quadratic emerges

$$9z^2 - 3(1-b)z - a + 2(1 + b + b^2) = 0 \tag{29}$$

for the two $P = 3$ cycles. The two solutions of (29) are

$$6z = 1 - b \pm \sqrt{\Delta_3}, \tag{30}$$

with

$$\Delta_3 \triangleq 4a - 7 - 10b - 7b^2 \geq 0, \tag{31}$$

defining the onset of real cycles for $P = 3$. Eq. (31) has already been discussed, without derivation, in [13, eq. (8)]. The curve $\Delta_3 = 0$ is shown in fig. 1 and is labeled 3.

Now, in order to distinguish the stable and unstable cycle, our solution is matched at $a = \frac{5}{4}$, $b = -1$ to a previously known solution [21] for a quadratic area-preserving map. It is found that the lower sign in (30) is appropriate for the stable cycle. Finally, with z known, the final expressions for α, β and γ are obtained in terms of a and b only,

$$2a\alpha = 1 - b - \sqrt{\Delta_3},$$
$$-2a^2\beta = 2a + (1 + 4b + b^2) + (1-b)\sqrt{\Delta_3}, \tag{32}$$
$$2a^3\gamma = a(1-b) - 2 - b + b^2 + 2b^3 + (a+b)\sqrt{\Delta_3}.$$

These will be needed below for the stability analysis.

The eigenvalue equation is constructed in the same way as previously for $P = 1$ and 2 and takes the form (7) with

$$\Sigma = 2a(b\alpha + 4a^2\gamma), \tag{33}$$

where α and γ are to be replaced by their expressions in (32).

Setting $\lambda = -1$ in the eigenvalue equation, we can obtain an equation for the onset of $P = 6$; this is given by the only real solution of

$$\begin{aligned}&A^3 - 2(4 + b + 4b^2)A^2\\ &+ 9(2 - 6b - 7b^2 - 6b^3 + 2b^4)A\\ &- 9(9 + 6b + 2b^2 - 10b^3 + 2b^4 + 6b^5 + 9b^6) = 0,\end{aligned} \tag{34}$$

where $A \triangleq 4a$ for convenience. The boundary determined from (34), called $\Delta_6 = 0$ in analogy to the previous Δ_j, is also plotted in fig. 1 and is labeled 6. Now we use eq. (7) together with eqs. (31)–(33) to establish the region where both eigenvalues satisfy $|\lambda| < 1$. We find:

(i) The cycle corresponding to the + sign in (30) is always unstable.
(ii) The cycle corresponding to the − sign in (30) is stable between $\Delta_3 = 0$, $\Delta_6 = 0$ and $|b| = 1$; otherwise it is also unstable.

The regions for real and complex eigenvalues of $P = 3$ have also been determined by analyzing the discriminant $\Sigma^2/4 + b^3$ of (7). After some algebra, the onset of complex conjugate eigenvalues is given by the condition

$$(4a + 3b)\sqrt{\Delta_3} + 4a(1-b) - 8(1-b^3) - 3b(1-b) \pm 2b\sqrt{-b} = 0, \tag{35}$$

which determines the boundary of the shaded region shown in fig. 3. This region, in turn, is bounded by the two curves $\Delta_3 = 0$ and $\Delta_6 = 0$ given, respectively, by (31) and (34). Note that, by virtue of the last term in (35), complex conjugate eigenvalues exist only for $b \leq 0$ while, for $b > 0$, both λ_i are necessarily real. The single point solution of (35) for $b = 0$ is $a = 1.75487767\ldots$. A

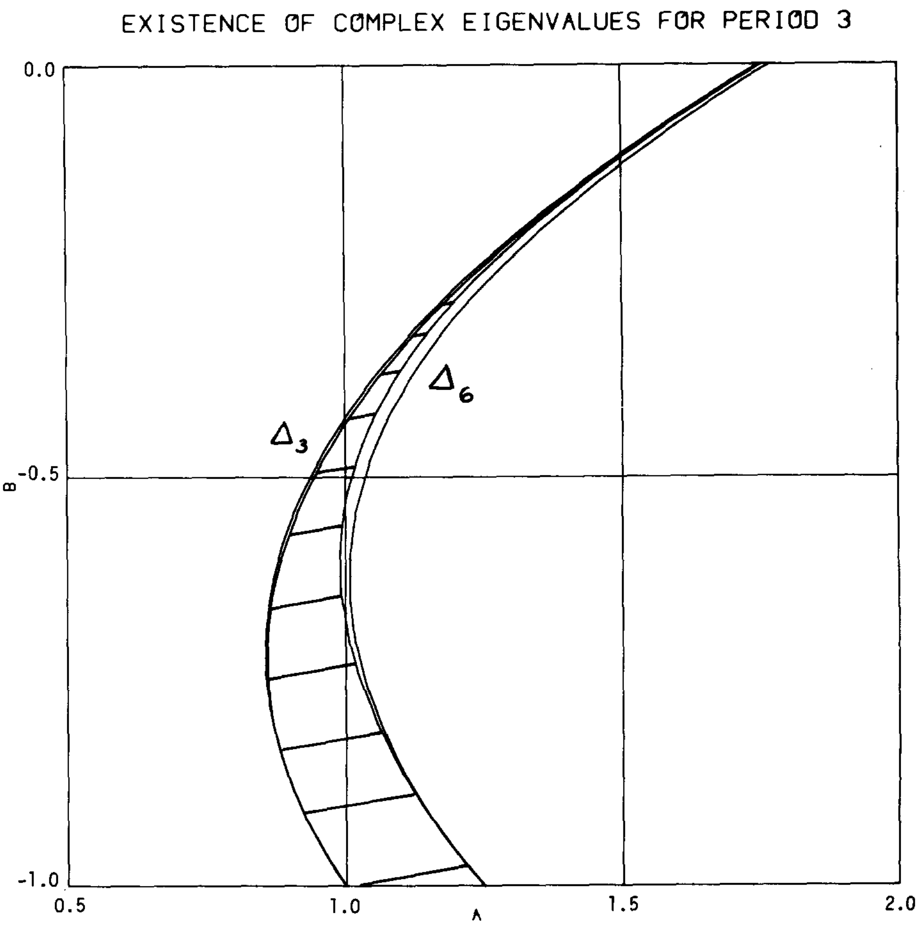

Fig. 3. Region for complex eigenvalues of period 3.

Table II
Emergence of stable cycles of periods 3 and 6

Period	a	b	x_0	x_1	x_2
3	6.0	1.0	0.50	−0.50	0.0
6	6.0	1.0	0.50	−0.50	0.0
3	3.4375	0.5	0.6881	−0.6234	0.0079
6	3.4408	0.5	0.6869	−0.6260	−0.0049
3	2.6575	0.3	0.7537	−0.7189	0.0969
6	2.6645	0.3	0.7944	−0.6844	−0.0099
3	1.75	0.0	0.9983	−0.7440	0.0314
6	1.7685	0.0	0.9984	−0.7630	−0.0297
3	1.1575	−0.3	1.2078	−0.7063	0.0601
6	1.2090	−0.3	1.2219	−0.7765	−0.0955
3	0.9375	−0.5	1.2691	−0.5504	0.0814
6	1.0360	−0.5	1.3204	−0.7128	−0.1865
3	1.0	−1.0	1.0	0.0	0.0
6	1.25	−1.0	1.2	−0.4	−0.4

pattern has now emerged; the iterated map T^n with n odd has only real eigenvalues for $b > 0$.

Finally, appropriate data for the stable cycles of $P = 3$ and 6 is given in table II. We remark that the three fixed points, x_0, x_1 and x_2, are obtained directly from (24) and (32). In order to summarize the results achieved at this point, a second plot of the boundaries for $P = 1$ to 4 is given in fig. 4 on an expanded scale with $-1 \leq b \leq 1$. Note that the structure in the a, b plane is somewhat complicated [22; first letter] and that we already see regions where, for example, cycles of $P = 1$ and $P = 3$ both exist or cycles of $P = 2$ and $P = 3$ coexist. We now proceed, the reader willing (!), to $P = 4$.

5. Period 4 fixed points

For a cycle of period 4, there are now $2^4 = 16$ total fixed points; two belong to $P = 1$ repeated four times and two belong to $P = 2$ repeated twice. The remaining twelve then form three separate cycles of $P = 4$. These are the cycles we will now investigate.

To begin, we note that, depending upon the nature of the governing equations (3), (10) or (21), the analysis to determine the existence of real cycles has proceeded in a different way for each of the periods 1 to 3. As a result of the earlier success with $P = 3$, the same approach based upon the elementary symmetric functions was applied to $P = 4$. This approach was successful and a cubic equation $C(z, a, b) = 0$ was obtained for the three unknown $P = 4$ cycles. Here z is defined by (12). However, an immense amount of algebraic labor [23 and 22; second letter] was required – the desired cubic polynomial was determined by factoring a tenth order polynomial! Thus, an alternate approach based upon the discrete Fourier Transform will be described here. This technique, communicated to us by Tassos Bountis [24] is so simple and elegant that the way was then opened to attack the problem of determining real cycles for both $P = 5$ and 6 analytically and in closed form!

The procedure is as follows. To solve for the unknown fixed points x_t, $t = 0, 1, 2, 3$, we set

$$x_t = \sum_{n=-1}^{2} A_n e^{in\omega t}, \tag{36}$$

where $i = \sqrt{-1}$ and $\omega = 2\pi/4 = \pi/2$. Then the four complex coefficients A_n are to be determined. This is done by inserting (36) into the two-step recurrence (2) and equating coefficients of $e^{in\omega t}$. If we define

$$A_1 \triangleq r e^{i\phi} \equiv \bar{A}_{-1}, \tag{37}$$

the following four nonlinear algebraic equations are obtained:

$$\begin{aligned} &A_0(1-b) = 1 - a\left(A_0^2 + A_2^2\right) - 2ar^2, \\ &A_2(1 - b - 2aA_0) = 2ar^2 \cos 2\phi, \\ &2a(A_0 + A_2)\cos\phi = (1+b)\sin\phi, \\ &2a(A_2 - A_0)\sin\phi = (1+b)\cos\phi, \end{aligned} \tag{38}$$

for the four unknowns A_0, A_2, r and ϕ. In

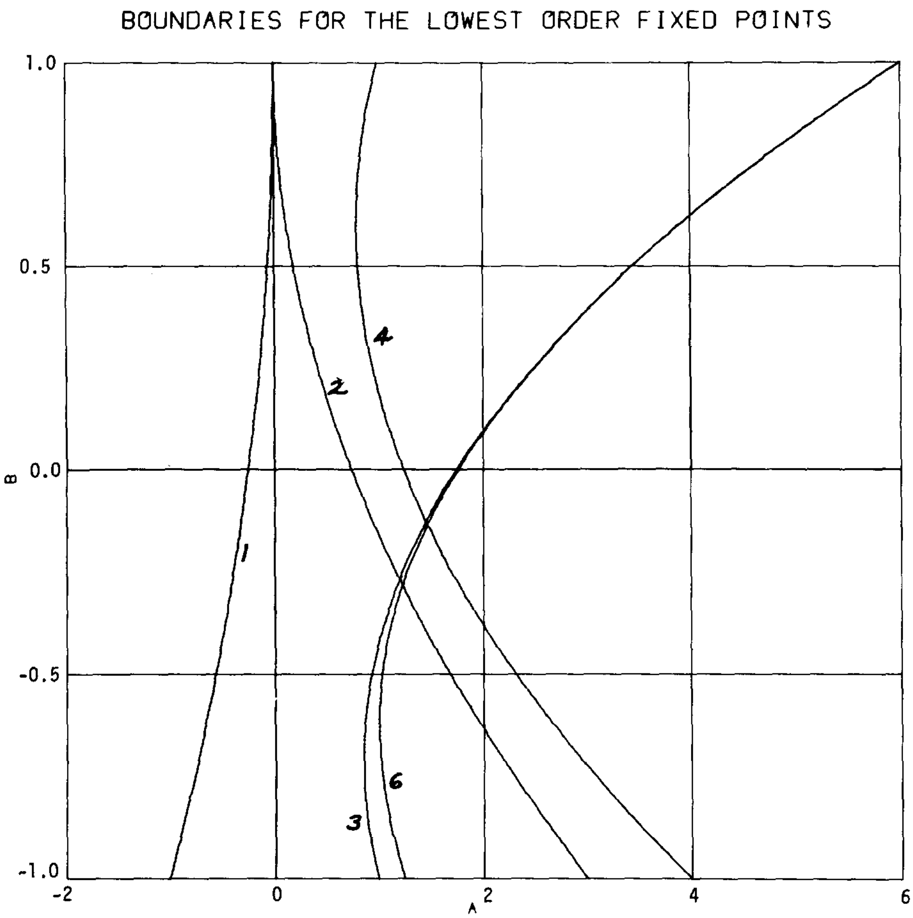

Fig. 4. Boundaries for the onset of real stable cycles of periods 1, 2, 3, 4, and 6. (Enlargement of fig. 1).

particular, the third and fourth equations in (38) yield

$$\tan\phi = \frac{2a(A_0 + A_2)}{1+b} = \frac{1+b}{2a(A_2 - A_0)}, \tag{39}$$

so

$$4a^2A_2^2 = 4a^2A_0^2 + (1+b)^2. \tag{40}$$

Next, with z defined by eq. (12), we find

$$z = aA_0 \tag{41}$$

and the desired cubic equation

$$16z^3 - \left[4a - 3(1+b)^2\right]z - (1-b)(1+b)^2 = 0 \tag{42}$$

is easily obtained after the variables ϕ, A_2 and r are eliminated. Given a and b, we can readily solve (42) for real values of z; for real cycles (i.e., real values of x_t) we have one further restriction [23; third letter]

$$a \geq 2z^2 + (1-b)z + \tfrac{1}{4}(1+b)^2 \tag{43}$$

which occurs since r [defined in (37)] must satisfy

$r \geq 0$. Then, using eqs. (36) and (37), we can express the four real fixed points x_t in the following form:

$$\begin{aligned} x_0 &= A_0 + A_2 + 2r\cos\phi, \\ x_1 &= A_0 - A_2 - 2r\sin\phi, \\ x_2 &= A_0 + A_2 - 2r\cos\phi, \\ x_3 &= A_0 - A_2 + 2r\sin\phi. \end{aligned} \tag{44}$$

With the fixed points x_t now known as a function of a and b, the eigenvalue equation $|M - \lambda I| = 0$ is given by (7) with

$$\Sigma = -16a^4 x_0 x_1 x_2 x_3 - 4a^2 b(x_0 x_1 + x_0 x_3 + x_1 x_2 + x_2 x_3) - 2b^2. \tag{45}$$

Then, putting $\lambda = \pm 1$ in (7), we obtain the defining equations for the emergence of stable cycles for $P = 4$ and 8 as

$$\begin{aligned} g(\lambda = +1) &= \Sigma + 1 + b^4 = 0, \\ h(\lambda = -1) &= -\Sigma + 1 + b^4 = 0. \end{aligned} \tag{46}$$

Note, however, that $h(\lambda = -1) = 0$ only gives the period doubling solutions for $P = 8$.

Since the cubic equation (42) contains both a and b as parameters, eqs. (46) together with (42) were solved numerically using the Univac 1110 computer by specifying the parameter b and iterating on the remaining parameter a. The resulting stability boundaries in the a, b plane are shown in fig. 5. Note that there are at most two stable $P = 4$

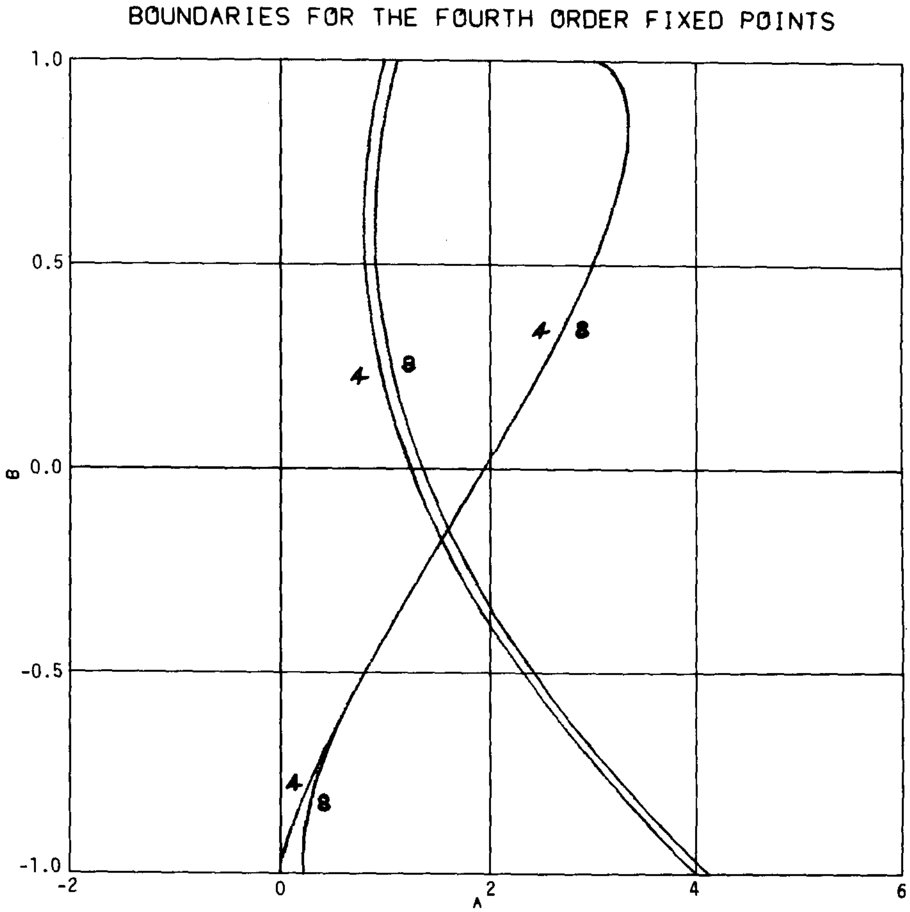

Fig. 5. Boundaries for the emergence of real stable cycles of periods 4 and 8.

cycles which occur in two thin bands; the second band on the right for $b > 0$ is very narrow. The left-hand curve for $b > 0$ is simply $\Delta_4 = 0$ given by (18) and shown previously in figs. 1, 2 and 4. The curve to its immediate right labelled 8 is, of course, $\Delta_8 = 0$ and shows where the stable $P = 4$ cycle bifurcates to $P = 8$.

In order to facilitate comparison, figs. 4, 5 and the forthcoming figs. 7, 8 are all plotted on the same scale. Clear plastic overlays are available from the first author so the reader can examine the various boundaries in different combinations.

In fig. 5, the second curve for $P = 4$ starting at $a = 0$, $b = -1$ and going to $a = 3$, $b = 1$ marks the onset of a second, stable cycle for $P = 4$. This curve is also known analytically. Returning to the fundamental cubic for $P = 4$ given by (42), the condition for the onset of 3 real values of z (hence, the possibility of 3 real cycles for $P = 4$) is given by

$$A^3 - 9(1+b)^2 A^2 + 27(1+b)^4[A - 5 + 6b - 5b^2] = 0, \tag{47}$$

where, as in (34), $A \triangleq 4a$ for simplicity. The single real solution of (47) is

$$4a = 3(1+b)\left[1 + b + \sqrt[3]{4(1-b)^2(1+b)}\right] \tag{48}$$

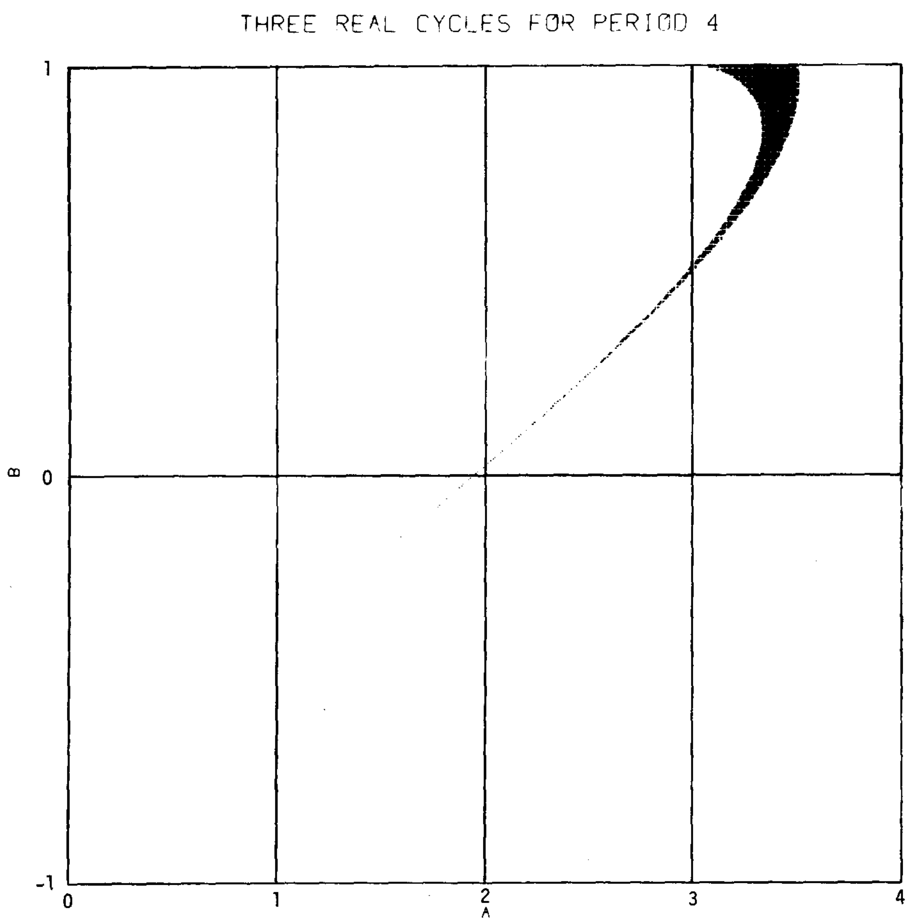

Fig. 6. Region where three real cycles of period 4 exist. At most, only one cycle will be stable.

Table III
Emergence of stable cycles of periods 4 and 8

Period	a	b	x_0	x_1	x_2	x_3
4	1.0	1.0	1.0	−1.0	1.0	−1.0
8	1.1340	1.0	1.2046	−1.2046	0.5591	−0.5591
4	3.0	1.0	0.8047	−0.8047	−0.1381	0.1381
8	3.1705	0.98	0.7618	−0.7905	−0.2349	0.0504
4	0.8125	0.5	1.2810	−0.6657	1.2804	−0.6650
8	0.9208	0.5	1.4081	−0.9335	0.9018	−0.2155
4	2.9753	0.5	0.7762	−0.7852	−0.4464	0.0145
8	2.9758	0.5	0.7756	−0.7855	−0.4482	0.0094
4	0.9125	0.3	1.1927	−0.4256	1.1925	−0.4253
8	1.0259	0.3	1.2706	−0.6744	0.9146	−0.0605
4	2.5992	0.3	0.8395	−0.8289	−0.5340	0.0101
8	2.5997	0.3	0.8391	−0.8293	−0.5362	0.0037
4	1.25	0.0	0.9658	−0.1658	0.9656	−0.1655
8	1.3681	0.0	0.9949	−0.3542	0.8284	0.0611
4	1.9406	0.0	0.9999	−0.9403	−0.7157	0.0060
8	1.9415	0.0	0.9999	−0.9412	−0.7198	−0.0060
4	1.2489	−0.3	1.3109	−1.1470	−1.0364	0.0027
8	1.2512	−0.3	1.3133	−1.1496	−1.0474	−0.0278
4	1.8125	−0.3	0.7660	−0.0488	0.7659	−0.0486
8	1.9217	−0.3	0.7733	−0.1745	0.7095	0.0850
4	0.8066	−0.5	1.7263	−1.4038	−1.4526	−0.0002
8	0.8123	−0.5	1.7355	−1.4089	−1.4803	−0.0757
4	2.3125	−0.5	0.6662	−0.0176	0.6662	−0.0175
8	2.4137	−0.5	0.6667	−0.1125	0.6361	0.0796
4	0.0	−1.0	0.0	0.0	1.0	1.0
8	0.2174	−1.0	4.9325	−2.1447	−4.9325	−2.1447
4	4.0	−1.0	0.5	0.0	0.5	0.0
8	4.0794	−0.99	0.4953	−0.0601	0.4950	0.0601

and was found to match the second boundary for $P = 4$ shown in fig. 5. Thus, to the left of the two intersecting curves labelled 4 in fig. 5, there is no real cycle of $P = 4$ while, to the right, there is at least one real cycle. These cycles are only stable between the boundaries shown and $|b| = 1$.

The allowable region in the a, b plane for three real $P = 4$ cycles is shown in fig. 6. This region begins where the two curves given by eqs. (18) and (48) cross. This intersection point can be determined exactly by noting that the term in brackets in (47) is Δ_4. So, along $\Delta_4 = 0$, we obtain the simultaneous equations

$$A = 9(1+b)^2 = 5 - 6b + 5b^2 \tag{49}$$

which yield the desired intersection point

$$b = -3 + 2\sqrt{2} = -0.1715\ldots,$$
$$a = 1.5441\ldots.$$

If we compare figs. 5 and 6, it is seen that over almost all of the region shown in fig. 6, all three real cycles are unstable. From fig. 5 we see that there exists either 0, 1 or 2 stable cycles of $P = 4$; one of the three cycles is always unstable. Data for the bounding stable cycles of both $P = 4$ and $P = 8$ is presented in table III together with numerical values for the four fixed points x_0, x_1, x_2 and x_3.

6. Period 5 fixed points

For a cycle of period 5, there are $2^5 = 32$ total fixed points; two belong to $P = 1$ repeated five times while the remaining thirty form six separate cycles of $P = 5$. These cycles will now be analyzed.

Because of the ease with which $P = 4$ was solved using the method of Tassos Bountis, the same approach was applied to $P = 5$. For this case, we set

$$x_t = \sum_{n=-2}^{2} A_n e^{in\omega t}, \tag{50}$$

with $\omega = 2\pi/5$. We find the variables A_1, A_{-1} and A_2, A_{-2} are complex conjugates so we define

$$\begin{aligned} A_1 &= \bar{A}_{-1} \triangleq r e^{i\zeta}, \\ A_2 &= \bar{A}_{-2} \triangleq s e^{i\eta}, \end{aligned} \tag{51}$$

together with the fundamental variable $z = aA_0$ according to (12). Note that both $r \geq 0$ and $s \geq 0$. By inserting (50) into (2), we obtain the following set of five nonlinear algebraic equations:

$$\begin{aligned} &z^2 + (1-b)z + 2a^2(r^2+s^2) - a = 0, \\ &(1+b)\sin\omega = as[\tau\sin\theta_1 + 2\sin\theta_2], \\ &2z + (1-b)\cos\omega = -as[\tau\cos\theta_1 + 2\cos\theta_2], \\ &(1+b)\sin 2\omega = ar[2\sin\theta_1 - \tau^{-1}\sin\theta_2], \\ &2z + (1-b)\cos 2\omega = -ar[2\cos\theta_1 + \tau^{-1}\cos\theta_2], \end{aligned} \tag{52}$$

for the unknowns z, r, s, ζ and η. Here

$$\begin{aligned} \theta_1 &\triangleq \zeta + 2\eta, \\ \theta_2 &\triangleq 2\zeta - \eta, \end{aligned} \tag{53}$$

and

$$\tau \triangleq s/r \geq 0$$

have also been defined so that eqs. (52) can be written quite compactly.

Next, a laborious algebraic reduction of (52) was undertaken and the unknowns θ_1, θ_2, r and s were eliminated in terms of a new variable $\rho \triangleq \tau^2 = \tau^2(z, b)$. If we skip all the algebra, a cubic equation in ρ is obtained with coefficients which are functions of z and b only. This equation can readily be solved for real positive values of ρ. Hence the five fixed points x_t are now known in terms of the two quantities z and b. If we return to eqs. (50) and (51), these fixed points have the following expressions:

$$\begin{aligned} x_0 &= z/a + 2r\cos\zeta + 2s\cos\eta, \\ x_1 &= z/a + 2r\cos(\zeta+\omega) + 2s\cos(\eta+2\omega), \\ x_2 &= z/a + 2r\cos(\zeta+2\omega) + 2s\cos(\eta-\omega), \\ x_3 &= z/a + 2r\cos(\zeta-2\omega) + 2s\cos(\eta+\omega), \\ x_4 &= z/a + 2r\cos(\zeta-\omega) + 2s\cos(\eta-2\omega). \end{aligned} \tag{54}$$

We proceed next to the stability analysis of these fixed points. Ultimately, of course, we want to develop a numerical algorithm to obtain the boundary curves in the a, b plane for the emergence of stable cycles of $P = 5$ and 10.

Since z is the remaining free variable, this is easily done by iterating on z using the eigenvalue equation (7). For $P = 5$, Σ is given by

$$\begin{aligned} \Sigma \triangleq\ & 32a^5x_0x_1x_2x_3x_4 + 8a^3b(x_0x_1x_2 + x_0x_1x_4 \\ & + x_0x_3x_4 + x_1x_2x_3 + x_2x_3x_4) + 10b^2z \end{aligned} \tag{55}$$

and, setting $\lambda = \pm 1$ in (7), we obtain the defining equations for the emergence of stable cycles of period 5

$$g(\lambda = +1) = \Sigma + 1 - b^5 = 0 \tag{56}$$

and for the emergence of period 10 by "pitchfork" bifurcation

$$h(\lambda = -1) = \Sigma - 1 + b^5 = 0. \tag{57}$$

These equations have been solved numerically on

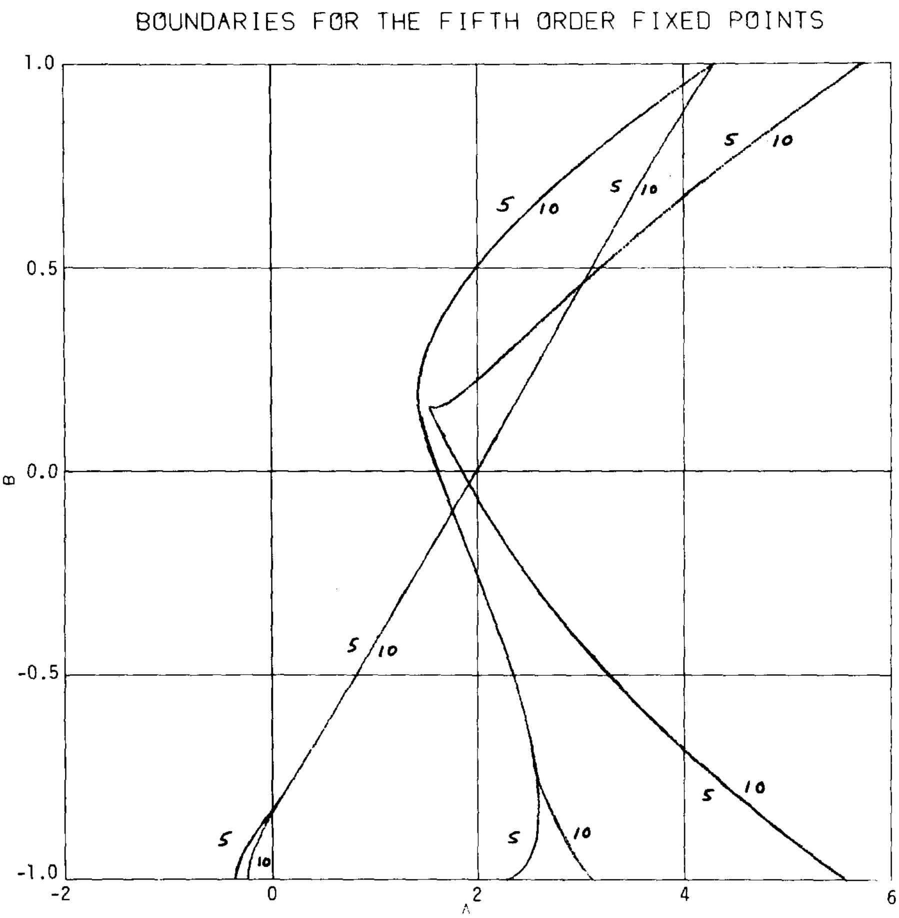

Fig. 7. Boundaries for the emergence of real stable cycles of periods 5 and 10.

the computer by iteration on the remaining free variable z. The results of this calculation, which was done using an error tolerance $\varepsilon = 1 \times 10^{-5}$, are the stability boundaries in the a, b plane shown in fig. 7. Note that, on the scale of this plot, the bands for stability are very thin so the boundary lines shown are actually double except for $b \leq -0.75$. For a fixed value of b, the boundary curve for $P = 5$ occurs first (for a slightly smaller value of a) before the boundary curve for $P = 10$ emerges.

If we first fix b and then increase a from small values (i.e., proceed to the right in fig. 7), we have 0, 2, 4 and 6 real cycles of $P = 5$ as the boundaries are crossed successively. Three of these cycles are always unstable. In the narrow bands we have one stable cycle whereas, at the four intersections of the boundary curves near $b = -0.09$, -0.03, 0.46 and 1.00, we have two identical stable $P = 5$ cycles.

Numerical data for a, b and the fixed points x_t is given in table IV for several selected values of b. In particular, the width of the band between $P = 5$ and 10 can be easily assessed using the data in this table. Note that, for each value of b, there are three stable cycles of period 5.

There is still one unresolved problem area however. The precise form of the "cusp" shown near $a \approx 1.593$, $b \approx 0.155$ is presently not understood [25]. Accurate and reliable numerical calculations are extremely difficult in this vicinity.

Table IV
Emergence of stable cycles of periods 5 and 10

Period	a	b	x_0	x_1	x_2	x_3	x_4
5	4.2946	1.0	0.6872	−0.6289	−0.0114	0.3705	0.3989
10	4.2948	1.0	0.6293	−0.6872	−0.3987	−0.3699	0.0135
5	4.2946	1.0	0.6872	−0.6289	−0.0114	0.3705	0.3989
10	4.2948	1.0	0.6293	−0.6872	−0.3987	−0.3699	0.0135
5	5.7274	1.0	0.5	−0.4319	0.4319	−0.5	0.0
10	5.7274	1.0	0.5	−0.4319	0.4319	−0.5	0.0
5	1.9888	0.5	1.0166	−0.8730	−0.0073	0.5634	0.3651
10	1.9893	0.5	1.0170	−0.8755	−0.0164	0.5617	0.3642
5	3.0980	0.5	0.7629	−0.7975	−0.5890	−0.4736	0.0107
10	3.0980	0.5	0.7626	−0.7975	−0.5892	−0.4744	0.0082
5	3.1871	0.5	0.6766	−0.4590	0.6669	−0.6469	−0.0001
10	3.1872	0.5	0.6768	−0.4591	0.6668	−0.6465	0.0014
5	1.5240	0.3	1.1451	−0.9336	0.0152	0.7196	0.2155
10	1.5275	0.3	1.1467	−0.9451	−0.0204	0.7158	0.2111
5	2.3265	0.3	0.7799	−0.4159	0.8316	−0.7337	−0.0029
10	2.3267	0.3	0.7804	−0.4162	0.8311	−0.7321	0.0023
5	2.6542	0.3	0.8369	−0.8565	−0.6961	−0.5432	0.0079
10	2.6543	0.3	0.8367	−0.8566	−0.6964	−0.5441	0.0053
5	1.6244	0.0	0.7785	0.0154	0.9996	−0.6231	0.3692
10	1.6284	0.0	0.7896	−0.0153	0.9996	−0.6272	0.3594
5	1.8606	0.0	0.9999	−0.8604	−0.3772	0.7353	−0.0059
10	1.8614	0.0	0.9999	−0.8611	−0.3803	0.7308	0.0058
5	1.9854	0.0	1.0	−0.9854	−0.9277	−0.7088	0.0024
10	1.9855	0.0	1.0	−0.9855	−0.9281	−0.7102	−0.0016
5	1.2956	−0.3	1.3133	−1.2335	−1.3651	−1.0443	−0.0034
10	1.2957	−0.3	1.3143	−1.2337	−1.3663	−1.0486	−0.0148
5	2.0666	−0.3	0.6202	0.0591	0.8067	−0.3626	0.4862
10	—	−0.3	—	—	—	—	—
5	2.6049	−0.3	0.8021	−0.6843	−0.4606	0.6528	0.0283
10	2.6050	−0.3	0.8019	−0.6845	−0.4609	0.6519	0.0314
5	0.8219	−0.5	1.7829	−1.6113	−2.0254	−1.5657	−0.0022
10	0.8220	−0.5	1.7889	−1.6117	−2.0296	−1.5802	−0.0377
5	2.3396	−0.5	0.5337	0.0829	0.7171	−0.2445	0.5016
10	—	−0.5	—	—	—	—	—
5	3.2593	−0.5	0.6934	−0.5842	−0.4590	0.6056	0.0343
10	3.2593	−0.5	0.6932	−0.5842	−0.4591	0.6052	0.0359
5	−0.5191	−1.0	0.4430	0.6589	0.7824	0.6589	0.4430
10	−0.2405	−1.0	−3.0755	1.6372	4.7201	4.7201	1.6372
5	2.2775	−1.0	0.3813	0.3229	0.3813	0.3460	0.3460
10	3.1262	−1.0	0.4299	−0.0077	0.5699	−0.0077	0.4299
5	5.5517	−1.0	0.4973	−0.4042	−0.4042	0.4973	0.3010
10	5.5517	−1.0	0.4972	−0.4042	−0.4042	0.4972	0.0316

7. Period 6 fixed points

The final analytical development to be presented here gives the algorithm which was formulated to determine the boundary curves in the a, b plane for $P = 6$ and their subsequent bifurcation to $P = 12$ when the eigenvalue $\lambda = -1$. For the cycle of period 6, there are $2^6 = 64$ total fixed points; 10 are redundant in the following ways:

2 belong to $P = 1$ repeated six times;
2 belong to $P = 2$ repeated three times;
6 belong to $P = 3$ repeated twice.

The remaining 54 fixed points then form 9 cycles of $P = 6$. Of these, we find at most 5 real stable cycles of period 6.

For $P = 6$, we write

$$x_k = \sum_{n=-2}^{3} A_n e^{in\omega k}, \tag{58}$$

with $\omega = 2\pi/6 = \pi/3$. Just as for $P = 4$ and 5, we find the unknown coefficients A_1, A_{-1} and A_2, A_{-2} are complex conjugates so eqs. (51) are again employed here. Again $z = aA_0$ and, inserting (58) into (2), the following set of six nonlinear algebraic equations is obtained:

$$\begin{aligned}
&z^2 + (1-b)z + 2a^2(r^2+s^2) + a^2A_3^2 - a = 0,\\
&\frac{\sqrt{3}}{4}(1+b) = as\left[\frac{A_3}{r}\sin\theta_1 - \sin\theta_2\right],\\
&4z + (1-b) = -4as\left[\frac{A_3}{r}\cos\theta_1 + \cos\theta_2\right],\\
&A_3(1-b-2z) = 4ars\cos\theta_1 \qquad\qquad (59)\\
&\frac{\sqrt{3}}{2}(1+b) = a\left[s\sin 3\eta + 2\frac{r}{s}A_3\sin\theta_1 + \frac{r^2}{s}\sin\theta_2\right],\\
&-4z + (1-b) = 2a\left[s\cos 3\eta + 2\frac{r}{s}A_3\cos\theta_1 + \frac{r^2}{s}\cos\theta_2\right],
\end{aligned}$$

for the unknowns z, r, s, A_3, ζ and η. In eqs. (59) we have also used the definitions

$$\begin{aligned}
\theta_1 &\triangleq \eta + \zeta,\\
\theta_2 &\triangleq \eta - 2\zeta,
\end{aligned} \tag{60}$$

so $3\eta = 2\theta_1 + \theta_2$.

At this point, the parameter a is also unknown but we shall use the eigenvalue equation later to obtain one additional relation. Now, in order to simplify eqs. (59), some additional definitions are made

$$t \triangleq aA_3, \quad u \triangleq ar, \quad v \triangleq as, \tag{61}$$

so the following two key variables:

$$\sigma \triangleq A_3/r \equiv t/u$$

and

$$\tau \triangleq s/r \equiv v/u \geq 0 \tag{62}$$

are obtained. Eq. (59) can then be expressed easily in terms of the unknowns σ, τ, z, v, θ_1 and θ_2. If we eliminate the three unknowns v, θ_1 and θ_2, an elaborate algebraic reduction of the last five equations in (59) yields two implicit equations $H_1 = 0$, $H_2 = 0$ in terms of the remaining three unknowns σ, τ and z. The parameter a is then determined from the first equation in (59) as follows:

$$a = 2v^2\left[1 + \tau^{-2}\left(1 + \tfrac{1}{2}\sigma^2\right)\right] + z^2 + (1-b)z, \tag{63}$$

so, in principal, the six fixed points x_k are now known in terms of the three quantities σ, τ and z. Using (58), six equations similar to those in (54) can be written for the x_k.

We proceed next to the stability analysis; the eigenvalue equation (7) can also be expressed in terms of σ, τ, z together with λ. For $P = 6$, Σ is given by

$$\begin{aligned}\Sigma \triangleq & -64a^6x_0x_1x_2x_3x_4x_5 \\ & -16a^4b(x_0x_1x_2x_3+x_0x_1x_4x_5 \\ & +x_0x_1x_2x_5+x_0x_3x_4x_5 \\ & +x_1x_2x_3x_4+x_2x_3x_4x_5) \\ & -4a^2b^2(x_0x_1+x_0x_3 \\ & +x_0x_5+x_1x_2+x_1x_4+x_2x_3 \\ & +x_2x_5+x_3x_4+x_4x_5)-2b^3. \end{aligned} \tag{64}$$

Putting $\lambda = \pm 1$ in (7), we obtain the final desired implicit relations for the emergence of $P = 6$,

$$g(\lambda = +1) = \Sigma + 1 + b^6 = 0, \tag{65}$$

and for the emergence of $P = 12$ by doubling,

$$h(\lambda = -1) = -\Sigma + 1 + b^6 = 0. \tag{66}$$

The implicit equations $H_1 = 0$, $H_2 = 0$, $g = 0$ and $h = 0$ just described have been solved numerically by a triple iteration in terms of the variables σ, τ and z. All the calculations were performed in double precision using the Univac 1110. The error tolerance ε was tightened to $\varepsilon = 1 \times 10^{-7}$ in comparison to $\varepsilon = 1 \times 10^{-5}$ used for $P = 5$ and 10 and

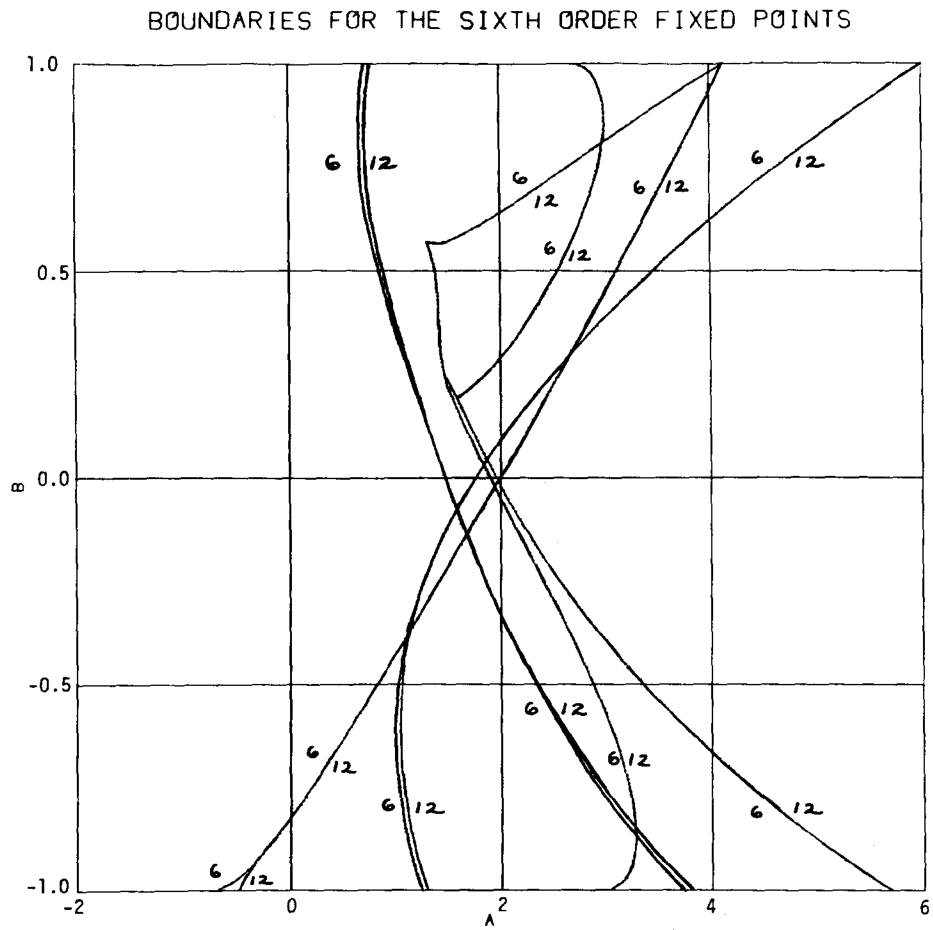

Fig. 8. Boundaries for the emergence of real stable cycles of periods 6 and 12.

Table V
Emergence of stable cycles of periods 6 and 12

Period	a	b	x_0	x_1	x_2	x_3	x_4	x_5
6	0.68086	0.95	1.1692	−0.8943	1.5662	−1.5197	0.9154	−1.0143
12	0.73706	0.95	0.9669	−0.4557	1.7655	−1.7304	0.4704	−0.8069
6	2.72577	1.0	0.8103	−0.6519	0.6519	−0.8103	−0.1379	0.1379
12	2.82024	0.99	0.7806	−0.6316	0.6476	−0.8079	−0.1999	0.0875
6	4.12402	1.0	0.4729	0.4302	0.7097	−0.6467	−0.0153	0.3523
12	4.12403	1.0	0.4729	0.4302	0.7096	−0.6467	−0.0149	0.3524
6	4.12402	1.0	−0.3523	0.0153	0.6467	−0.7097	−0.4302	−0.4729
12	4.12403	1.0	−0.3524	0.0149	0.6467	−0.7096	−0.4302	−0.4729
6	5.94018	0.99	−0.5022	−0.0001	0.5029	−0.5022	−0.0001	0.5029
6	4.61015	0.75	−0.5584	−0.0017	0.5812	−0.5584	−0.0017	0.5812
12	4.61153	0.75	−0.5569	0.0046	0.5822	−0.5597	−0.0080	0.5799
6	0.84081	0.5	1.2772	−0.3111	1.5572	−1.1945	0.5790	0.1209
12	0.86002	0.5	1.2111	−0.1692	1.5809	−1.2341	0.4805	0.1845
6	1.39376	0.5	0.7555	0.2369	1.2996	−1.2354	−0.4773	0.0647
12	1.39500	0.5	0.7515	0.2337	1.2996	−1.2391	−0.4920	0.0428
6	2.53866	0.5	0.7650	−0.4797	0.7984	−0.8579	−0.4693	0.0120
12	2.53868	0.5	0.7652	−0.4797	0.7983	−0.8578	−0.4688	0.0131
6	3.09608	0.5	−0.4703	0.0093	0.7646	−0.8052	−0.6249	−0.6115
12	3.09608	0.5	−0.4704	0.0090	0.7642	−0.8052	−0.6249	−0.6116
6	3.44076	0.5	−0.6260	−0.0049	0.6869	−0.6260	−0.0049	0.6869
12	3.44291	0.5	−0.6231	0.0057	0.6883	−0.6284	−0.0154	0.6850
6	1.06237	0.3	1.0805	−0.1439	1.3021	−0.8445	0.6330	0.3210
12	1.07107	0.3	1.0499	−0.0753	1.3089	−0.8575	0.6051	0.3506
6	1.44923	0.3	0.8035	0.0751	1.2329	−1.1802	−0.6488	0.0359
12	1.45081	0.3	0.8009	0.0712	1.2329	−1.1839	−0.6636	0.0059
6	2.03977	0.3	0.8233	−0.3810	0.9509	−0.9586	−0.5890	0.0049
12	2.03985	0.3	0.8235	−0.3811	0.9508	−0.9582	−0.5878	0.0078
6	2.66201	0.3	−0.5421	0.0064	0.8373	−0.8642	−0.7368	−0.7045
12	2.66201	0.3	−0.5422	0.0060	0.8372	−0.8642	−0.7368	−0.7045
6	2.66445	0.3	−0.6844	−0.0099	0.7944	−0.6844	−0.0099	0.7944
12	2.66806	0.3	−0.6789	0.0078	0.7962	−0.6889	−0.0275	0.7913
6	1.47470	0.0	0.8305	−0.0170	0.9996	−0.4734	0.6695	0.3391
12	1.47974	0.0	0.8153	0.0163	0.9996	−0.4786	0.6611	0.3533
6	1.76853	0.0	−0.7630	−0.0297	0.9984	−0.7630	−0.0297	0.9984
12	1.77722	0.0	−0.7455	0.0122	0.9997	−0.7763	−0.0710	0.9910
6	1.90725	0.0	0.7233	0.0023	1.0000	−0.9072	−0.5697	0.3809
12	1.90737	0.0	0.7249	−0.0023	1.0000	−0.9073	−0.5702	0.3798
6	1.96676	0.0	0.7135	−0.0012	1.0000	−0.9668	−0.8382	−0.3817
12	1.96680	0.0	0.7126	0.0012	1.0000	−0.9668	−0.8383	−0.3823
6	1.99638	0.0	−0.7076	0.0004	1.0000	−0.9964	−0.9819	−0.9249
12	1.99638	0.0	−0.7079	−0.0004	1.0000	−0.9964	−0.9819	−0.9249
6	1.20899	−0.3	−0.7765	−0.0955	1.2219	−0.7765	−0.0955	1.2219
12	1.22858	−0.3	−0.7210	0.0005	1.2163	−0.8177	−0.1864	1.2026
6	1.30946	−0.3	−1.0423	−0.0099	1.3126	−1.2530	−1.4495	−1.3754
12	1.30947	−0.3	−1.0430	−0.0118	1.3127	−1.2530	−1.4496	−1.3756
6	1.94902	−0.3	0.6711	0.0431	0.7951	−0.2449	0.6446	0.2637
12	1.95554	−0.3	0.6585	0.0691	0.7931	−0.2509	0.6390	0.2768
6	2.50632	−0.3	0.5712	0.0367	0.8253	−0.7180	−0.5397	0.4855
12	2.50634	−0.3	0.5717	0.0352	0.8254	−0.7180	−0.5397	0.4853
6	2.69870	−0.3	0.6422	0.0278	0.8052	−0.7582	−0.7930	−0.4698
12	2.69871	−0.3	0.6421	0.0283	0.8052	−0.7582	−0.7931	−0.4699
6	0.83351	−0.5	−1.5766	−0.0240	1.7878	−1.6522	−2.1692	−2.0958
12	0.83353	−0.5	−1.5785	−0.0288	1.7886	−1.6521	−2.1693	−2.0964
6	1.03596	−0.5	−0.7128	−0.1865	1.3204	−0.7128	−0.1865	1.3204

Table V
(*continued*)

12	1.06213	−0.5	−0.6169	−0.0500	1.3058	−0.7861	−0.3092	1.2915
6	2.31776	−0.5	0.6004	0.0640	0.6903	−0.1365	0.6116	0.2012
12	2.32883	−0.5	0.5860	0.0911	0.6877	−0.1468	0.6060	0.2183
6	2.87586	−0.5	0.4890	0.0528	0.7475	−0.6332	−0.5267	0.5189
12	2.87587	−0.5	0.4894	0.0518	0.7476	−0.6332	−0.5267	0.5188
6	3.35250	−0.5	0.5997	0.0333	0.6964	−0.6426	−0.7326	−0.4782
12	3.35250	−0.5	0.5997	0.0335	0.6964	−0.6426	−0.7326	−0.4782
6	−0.61280	−0.99	1.2311	0.2526	−0.1797	0.7697	1.5410	1.6931
12	−0.45500	−0.98	2.3004	0.6025	−1.0892	0.9494	2.4776	2.8626
6	1.23766	−0.99	−0.4060	−0.3980	1.2060	−0.4060	−0.3980	1.2060
6	1.14080	−0.90	−0.4628	−0.3749	1.2562	−0.4628	−0.3749	1.2562
12	1.16974	−0.90	−0.3379	−0.2426	1.2353	−0.5665	−0.4871	1.2323
6	3.09838	−0.99	0.2648	0.1503	0.6679	−0.5310	−0.5350	0.6389
12	3.09876	−0.99	0.2674	0.1466	0.6687	−0.5308	−0.5351	0.6383
6	3.55687	−0.96	0.4870	0.0769	0.5115	−0.0043	0.5089	0.0830
12	3.59669	−0.96	0.4630	0.1139	0.5089	−0.0407	0.5055	0.1199
6	4.43516	−0.76	0.5451	0.0331	0.5808	−0.5214	−0.6473	−0.4620
12	4.43517	−0.76	0.5451	0.0332	0.5808	−0.5214	−0.6473	−0.4620

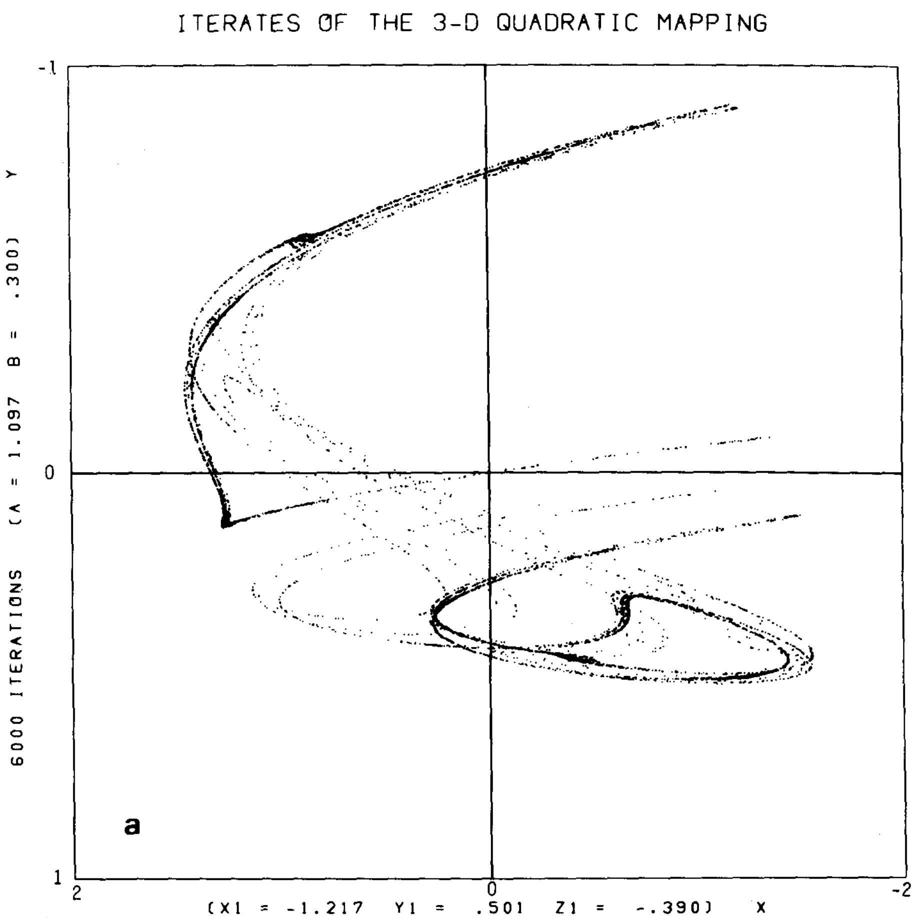

Fig. 9a. The x, y projection of the limiting strange attractor obtained with the 3-D quadratic map at $b = 0.3$.

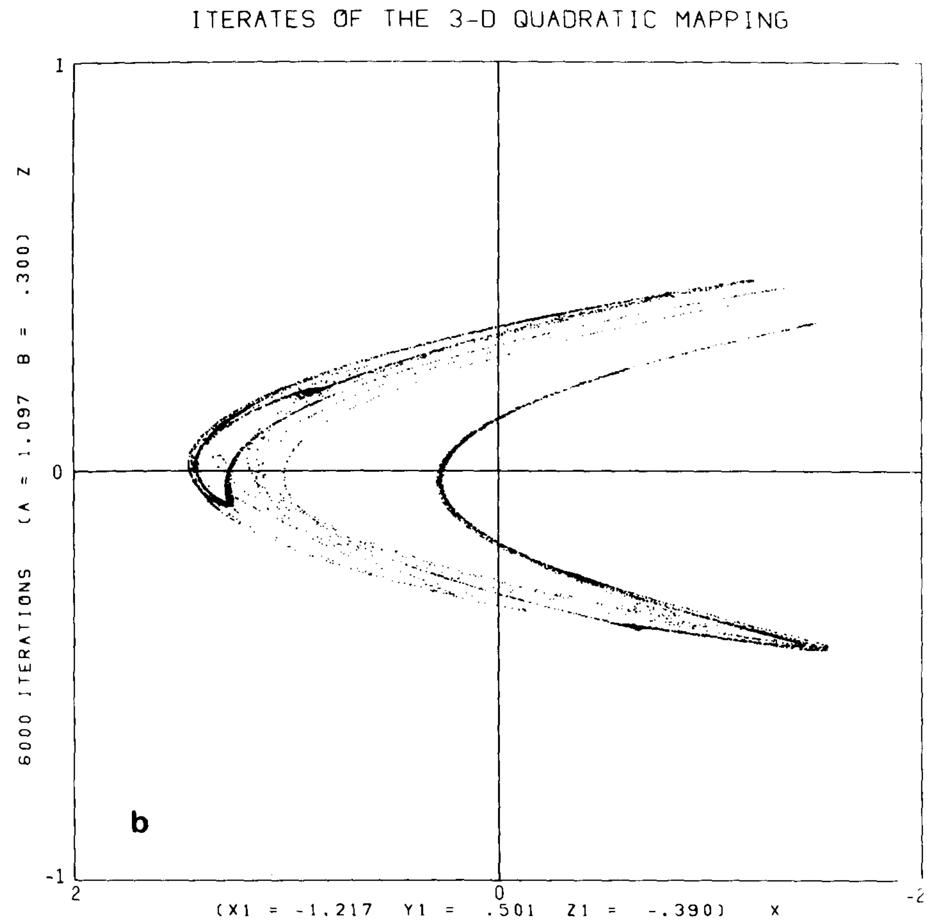

Fig. 9b. The x, z projection of the limiting strange attractor obtained with the 3-D quadratic map at $b = 0.3$.

$\varepsilon = 4 \times 10^{-5}$ used for $P = 4$ and 8. In particular, the root-sum-square (rss) of the errors in simultaneously satisfying $H_1 = 0$, $H_2 = 0$ and either $g = 0$ or $h = 0$ was required to be less than ε in magnitude. The results of this computation are shown in fig. 8. Note again that all the boundary curves are double on the scale of this plot – which scale is in fact the same as figs. 4, 5 and 7 so the boundary lines can be compared easily. In all cases, at a fixed value of b the boundary for $P = 6$ occurs first and then the boundary line for $P = 12$ emerges for a slightly larger value of a.

Numerical data for these bounding stable cycles of period 6 and 12 is given in table V. Values are tabulated for a, b and the fixed points $x_0, x_1, \ldots, x_5$. For the area-preserving limiting cases $b = \pm 1$, the numerical iteration is extremely delicate and did not always converge. For these two cases, some extra data is given which is "closest" to the desired value of b.

Since this was a numerical search based upon a triple iteration, we initially missed the left-most boundary curves in fig. 8 for $b > 0$. We are indebted to P.R. Stein [26] of LANL for pointing out this error in an earlier version of this paper.

This completes the analysis of the regions in the a, b parameter plane where real, stable cycles of periods 1 to 6 exist for the Hénon quadratic map.

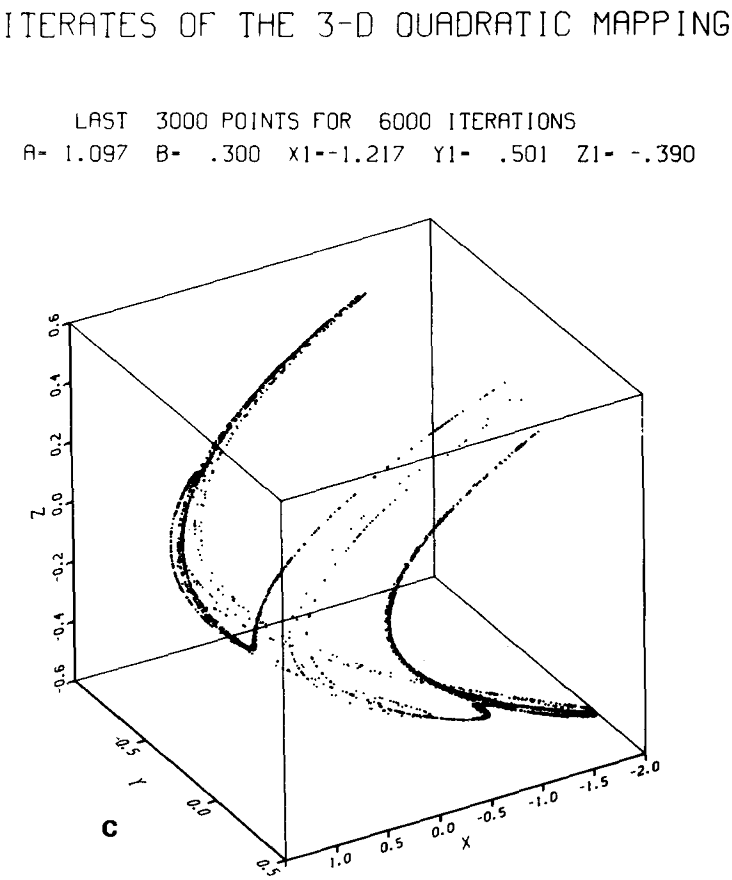

Fig. 9c. Three-dimensional isometric plot of the limiting strange attractor obtained at $b = 0.3$.

8. Generalization to three dimensions

In this final section, we want to briefly comment on one additional topic. Because of the marvelous attracting structures which can be generated using the incredibly simple two-dimensional Hénon quadratic map given in (1), we attempted to generalize the map to three-dimensions. The ground rules for this extension, which were somewhat arbitrary, were:

1) The nonlinearities would be, at most, quadratic;

2) the Jacobian J would remain equal to the same constant as the Hénon map – namely $J = -b$;

3) only the two parameters a and b were to enter.

Subject to these conditions, the three-dimensional map was given by

$$\begin{aligned} x_{i+1} &= 1 + y_i - a x_i^2, \\ y_{i+1} &= b x_i + z_i, \\ z_{i+1} &= -b x_i. \end{aligned} \tag{67}$$

Note, of course, that the three conditions above do not uniquely determine the map; for example, a term in z or z^2 could be added to the first equation above and the three conditions would still be satisfied.

This map was iterated on the computer and strange attractors were found in the three-dimensional x, y, z space. Two-dimensional projections of one of these attractors are shown in figs. 9a, b. At the chosen parameter value $b = 0.3$, this attractor is, in fact, the limiting attractor on the C/E boundary in the $a - b$ parameter plane for (67). In particular, strange attractors of one component were found in the range $1.07 \leq a \leq 1.097$ for $b = 0.3$. The reader should attempt to combine (visually) the two figures 9a, b into one object in three-dimensional space. Since this is not too easy, a three-dimensional isometric plot of the resulting strange attractor is presented in fig. 9c. In this plot, the object looks remarkably simple.

9. Conclusions

In conclusion, it is hoped that the results of this systematic exploration of the $a - b$ parameter plane will be of value in other studies of either the Hénon map or related maps. Furthermore, this study should serve as a useful illustration of the richness and complexity inherent in even very simple nonlinear problems.

Acknowledgements

It is a pleasure to thank Dr. M. Hénon for acquainting me with his work, for suggesting this study, and for his penetrating comments and questions over several years. Also, we wish to thank Mrs. L. Staley and Mrs. Vivian Satterfield for typing two versions of this paper.

References

[1] R.H.G. Helleman, in: Fundamental Problems in Statistical Mechanics, vol. 5, E.G.D. Cohen, ed. (North-Holland, Amsterdam, 1980), p. 165. (302 references in 23 categories.)
[2] R.H.G. Helleman and R.S. MacKay, in: Non-Equilibrium Phenomena in Statistical Mechanics, vol. 2, W. Horton, L. Reichl, V. Szebehely, eds. (Wiley, New York, 1981).
[3] D. Ruelle, Math. Intelligencer 2 (1980) 126.
[4] D.R. Hofstadter, Scientific American 245 (1981) 22.
[5] A.I. Mees, Dynamics of Feedback Systems (Wiley, New York, 1981) chap. 1 and sec. 2.7, p. 51.
[6] R.M. May, Nonlinear Problems in Ecology and Resource Management, Lecture Notes for Les Houches Summer School on "Chaotic Behavior of Deterministic Systems," July 1981. (72 references.)
[7] M. Hénon, Commun. Math. Phys. 50 (1976) 69.
[8] S.D. Feit, Commun. Math. Phys. 61 (1978) 249.
[9] C. Simó, J. Stat. Phys. 21 (1979) 465.
[10] J.H. Curry, Commun. Math. Phys. 68 (1979) 129.
[11] F.R. Marotto, Commun. Math. Phys. 68 (1979) 187.
[12] H. Daido, Prog. Theor. Phys. 63 (1980) 1190.
[13] D.L. Hitzl, Physica 2D (1981) 370.
[14] T.C. Bountis, Physica 3D (1981) 577.
[15] H. Mori and H. Fujisaka, Prog. Theor. Phys. 63 (1980) 1931.
[16] H. Froehling, J.P. Crutchfield, D. Farmer, N.H. Packard and R. Shaw, Physica 3D (1981) 605.
[17] J.H. Curry and J.A. Yorke, in: The Structure of Attractors in Dynamical Systems, Lecture Notes in Math., vol. 668, A. Dold and B. Eckmann, eds. (Springer, New York, 1978), p. 48.
[18] J.L. Kaplan and J.A. Yorke, in: Functional Differential Equations and Approximation of Fixed Points, Lecture Notes in Math., vol. 730 (Springer, New York, 1979), p. 204.
[19] D.G. Aronson, M.A. Chory, G.R. Hall and R.P. McGehee, in: New Approaches to Nonlinear Problems in Dynamics, P.J. Holmes, ed., SIAM Asilomar Conf. Proc. (1980) 339.
[20] W.A. Beyer and P.R. Stein, Adv. in Appl. Math. 3 (1982) 1.
[21] M. Hénon, Quart. App. Math. 27 (1969) 291.
[22] M. Hénon, letters to D.L. Hitzl, 24 April 1979 and 21 Nov. 1979.
[23] D.L. Hitzl, letters to M. Hénon, 2 Nov. 1979, 5 Dec. 1979, and 16 Oct. 1980.
[24] T.C. Bountis, private communication, Dec. 1979.
[25] W.A. Beyer, private communications at Dynamics Days, Jan. 1983 and Jan. 1984.
[26] P.R. Stein, letter to D.L. Hitzl, 17 March 1982.